Nonadiabatic atomic ionization by intense subcycle laser pulses

Jian Zheng, Enming Qiu, Yingchun Yang, and Qiang Lin*

Institute of Optics, Department of Physics, Zhejiang University, Hangzhou 310027, China

(Received 18 October 2011; published 27 January 2012)

The atomic photoionization by a subcycle linearly polarized laser pulse is studied with numerical solutions of the time-dependent Schrödinger equation for a hydrogenlike atom. In this regime, the presumption for the adiabatic ionization theories that atoms are ionized directly from an initial bound state to the continuum state will fail. The nonadiabatic ionization channels turn out to play important roles: the bound electrons can climb up the energy ladder and get ionized from a certain bound state other than the original one. This process leaves significant fingerprints in carrier-envelope-phase-sensitive phenomena like total ionization yield and momentum asymmetry of the photoelectrons. For the modeling of subcycle pulses, the inconsistency of the popular vector potential definition is noticed and a modified version with an analytic envelope is presented that is capable of describing pulses with arbitrary pulse width.

DOI: 10.1103/PhysRevA.85.013417 PACS number(s): 32.80.Rm, 42.65.Re, 42.65.Ky

I. INTRODUCTION

In recent years, the great progress in the generation of ultrashort laser pulses has made possible the shortest electromagnetic pulses which consist of one or less optical cycles (measured full width at half maximum of the pulse's envelope) [1,2]. From the terahertz band [3], to the visible spectrum [4,5] and the extreme ultraviolet band [6,7], the single-cycle pulses start a new era for ultrafast science. The theoretical description of the single-cycle pulses and their interaction with matter has caught the interests of many researchers [8–16].

Atomic photoionization by pulses with durations that are large compared with the period of the carrier frequency is a well-understood process that is similar to ionization by a continuous-wave field [17]. In this regime, the atomic-orbital frequency is higher than the optical frequency; thus, the atomic dipole follows adiabatically the oscillations of the external field. As a result, the ionization rate depends on the instantaneous electric field. In this case the ionization rate can be calculated by using the projection of the evolved Volkov state on the ground state, as is done in Keldysh-type theories [18], or by using the Landau-Dyhne formulation [19]. These adiabatic theories are built upon the presumption that atoms are ionized directly from an initial bound state to the continuum states.

On the other hand, when the pulse duration approaches the period of the carrier, nonadiabatic effects take place [20]. As a result, the laser pulse induces transitions between the bound atomic states. Because a portion of the particles could be captured in these states, suppression of the ionization of the atom has been reported [20,21].

In this paper, we study the photoionization in an intense linearly polarized subcycle laser pulse by solving the time-dependent Schrödinger equation (TDSE) numerically. The inconsistency of the vector-potential definition is discussed and an accurate theoretical description for subcycle pulses is presented. The results show that, in the subcycle regime, when the pulse duration decreases, the major ionization channel gradually changes from the adiabatic ionization channel to the nonadiabatic one. This process leaves important fingerprints in carrier-envelope-phase (CEP)-sensitive observables, such as the ionization yield and the momentum asymmetry of photoelectrons as identified in the paper. Since these phenomena have been used as effective ways to determine the CEPs of few-cycle pulses [22,23], in the case that a determination of the CEPs for subcycle pulse is required, the effects discussed in this paper should be taken into account.

II. THE DESCRIPTION OF SUBCYCLE PULSE

The dc component in the carrier-envelope (CE) model with an envelope multiplied by a carrier wave is found to cause nonphysical results [15,16]. So, largely, the vector potential definition has been used instead to cancel out the dc part. It starts by defining the vector potential $A(t)$ as

$$A(t) = \mathrm{Re}\left[-\frac{c}{i\omega_0}E_0 f(t)\exp(i\omega_0 t + i\phi_0)\right], \qquad (1)$$

where $\omega_0 = 2\pi/T_0$ is the carrier frequency, T_0 is the period, ϕ_0 represents the absolute phase or CEP, E_0 is the amplitude, and $f(t)$ is a real Gaussian-like envelope function. The electric field is then derived as the first derivative of the vector potential. As long as the envelope function $f(t)$ satisfies

$$\lim_{t\to\pm\infty} f(t) = 0, \qquad (2)$$

the E field is guaranteed to have a zero dc component.

However, having a zero dc component is only a minimal requirement. Not all the assumed envelopes are physically meaningful: $f(t)$ is only physically meaningful as long as the spectrum content remains invariant under the change of its CEP [15]. Since a phase shift should not change its Fourier spectrum $E(\omega)$, the weighted center frequency $\omega_c = \int_0^\infty \omega|E(\omega)|^2 d\omega / \int_0^\infty |E(\omega)|^2 d\omega$ should remain unchanged when the CEP changes. As revealed by Fig. 1, the vector potential model remains at high accuracy for pulse durations down to three quarter cycles ($\tau_p \approx 0.75T_0$) for the four popularly used envelope functions, but fails for even shorter ones. The pulse width τ_p is defined as the full width at half maximum (FWHM) of $|f(t)|^2$. The above checking procedure

*qlin@zju.edu.cn

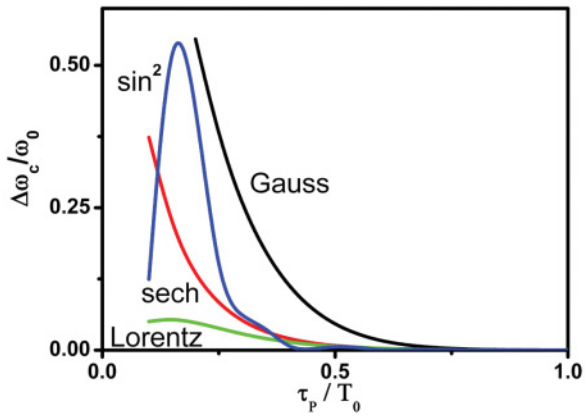

FIG. 1. (Color online) Phase dependence of the center frequency difference $\Delta\omega_c/\omega_0 = |\omega_c(\phi = 0) - \omega_c(\phi = \pi/2)|/\omega_0$ vs the normalized pulse duration for various pulse shapes; the envelopes are given by a $\sin^2$ with $f(t) = \sin^2[\pi t/(2.75\tau_p)]$ $(0 < t < 2.75\tau_p)$, a Gaussian with $f(t) = \exp[-(1.17t/\tau_p)^2]$, a hyperbolic secant with $f(t) = \mathrm{sech}(1.76t/\tau_p)$, and a Lorentzian with $f(t) = 1/[1 + (1.29t/\tau_p)^2]$.

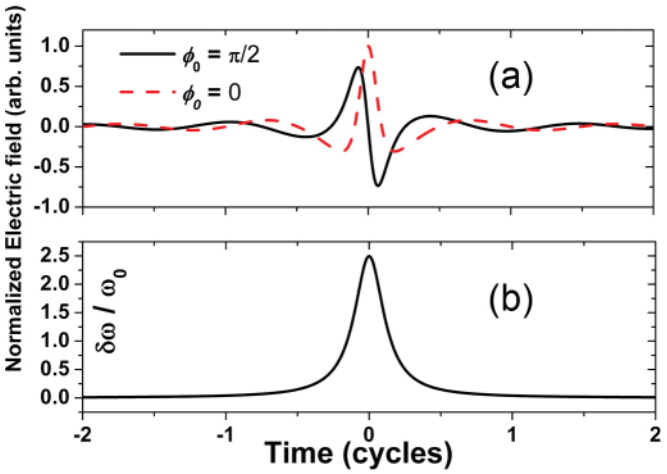

FIG. 2. (Color online) (a) Quarter-cycle waveforms with different CEPs ($\phi = 0$ and $\phi = \pi/2$) and (b) their relative frequency shift $\delta\omega/\omega_0$ vs time for the Lorentzian analytic envelope function $\tilde{f}(t) = 1/(1 - 2it/\tau_p)$.

is similar to that used in Ref. [15]. The reason why the vector-potential definition works in the long pulse limit but fails when the pulse is short enough could be explained by the Bedrosian theory.

To cover the whole range of pulse widths, we can modify the vector-potential definition by assuming $f(t)$ to be an analytic envelope $\tilde{f}(t) = u(t) + i\hat{u}(t)$, where real functions $u(t)$ and $\hat{u}(t)$ make up a Hilbert transform pair. By doing this, the derived E field expression becomes an analytic function and, as long as the dc part is removed, an analytic function will always fulfill the condition that its spectrum content remains invariant under the change of its CEP by its definition.

By taking a first time derivative, the E field could be derived and normalized to be

$$E(t) = \mathrm{Re}[E_0|A_d(0)|^{-1}A_d(t)\tilde{f}(t)\exp(i\omega_0 t + i\phi_0)]. \quad (3)$$

The expression has a similar structure to the CE expression except for the self-modulation factor $|A_d(0)|^{-1}A_d(t)$. The function

$$A_d(t) = 1 - i\frac{\dot{\tilde{f}}}{\omega_0\tilde{f}} \quad (4)$$

is the self-modulation function, where $\dot{\tilde{f}}$ is the first time derivative of $\tilde{f}(t)$. At the slow-varying-envelope limit, where the change of the envelope is much slower compared to the rapid oscillating carrier wave, $\dot{\tilde{f}}/\omega_0 \to 0$ and the expression reduces to the standard CE expression with $|A_d(0)|^{-1}A_d(t) = 1$. The total phase of this pulse is expressed as follows:

$$\phi(t) = \omega_0 t + \phi_0 + \arg[\tilde{f}(t)] + \arg[A_d(t)]. \quad (5)$$

The last two terms cause this transform-limited pulse to chirp intrinsically, which has been verified experimentally to exist in subcycle terahertz pulses [24].

Figure 2 shows the typical waveforms with different CEPs [Fig. 2(a)] and their relative frequency shift [Fig. 2(b)] for a Lorentzian analytic envelope with $\tilde{f}(t) = 1/(1 - 2it/\tau_p)$. Unless otherwise noted, this envelope is used throughout the paper.

III. THE THEORETICAL MODEL AND SIMULATION RESULTS

For a hydrogenlike atom interacting with a subcycle laser pulse linearly polarized along the x axis, the Hamiltonian in atomic units is given by

$$H = \left[-\frac{1}{2}\frac{\partial^2}{\partial x^2} + V(x) - E(t)x\right], \quad (6)$$

where $V(x) = -1/\sqrt{1 + x^2}$ is the Coulomb potential with soft core. The TDSE is solved numerically by the split-operator method [25] with the initial wave function being obtained by imaginary time propagation. The maximal grid point is taken to be 960 a.u. with a grid spacing of $\Delta x = 0.25$ a.u. and time propagation step to be $\Delta t = 0.03$ a.u.. A $\cos^{1/2}$-like absorbing mask function is used to avoid the reflections from the boundaries. The numerical simulation is performed until the final time t_f that is 50 times larger than the width of the pulse under consideration, so the slowest ionization signal could be collected. Since we are interested in the ionization signal measure in forward (P_+) and backward (P_+) directions along the polarization axis, the following integration of the probability flux near the absorbing boundaries (at x_+ for P_+, and x_- for P_-) is performed during the simulation:

$$\begin{aligned} P_+ &= \int_0^{t_f} j_{x_+}(t)dt, \\ P_- &= \int_0^{t_f} j_{x_-}(t)dt, \end{aligned} \quad (7)$$

where

$$j_x(t) = \mathrm{Re}\left[-i\Psi(x,t)^*\frac{\partial}{\partial t}\Psi(x,t)\right] \quad (8)$$

and $\Psi(x,t)$ is the wave function. The asymmetry coefficient a is defined as

$$a = (P_+ - P_-)/(P_+ + P_-) \tag{9}$$

and the total ionization probability reads $P = P_+ + P_-$.

This one-dimensional model is used throughout the paper. Such a model could overestimate the total ionization probability [26] and exaggerate the Coulomb effects by forcing the electron wave packet to "see" the core every time it returns. However, compared to a fully three-dimensional calculation, it can give qualitative pictures with much less time cost.

A. The total ionization probability versus CEP

With $E_0 = 0.08$ a.u. (corresponding to an intensity of 2.3×10^{14} W/cm^2) and the carrier wavelength of 800 nm, we calculated the total ionization probability as a function of CEP for different pulse width. The results are shown in Fig. 3(a) and are compared to the adiabatic ionization probability which is calculated using the quasistatic approximation for tunneling ionization for a hydrogen atom in its ground state. As discussed

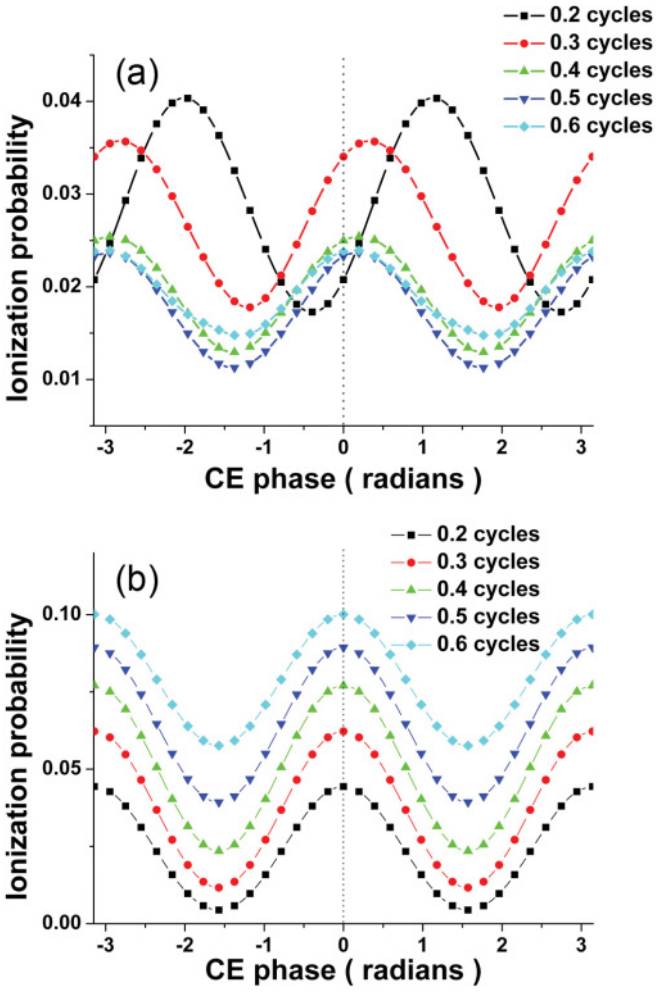

FIG. 3. (Color online) The total ionization probability vs CEPs for a hydrogenlike atom at ground state interacting with intense subcycle pulses with pulse width changing from 0.2 cycles to 0.6 cycles. (a) The TDSE results are compared to (b) those calculated with quasistatic tunneling rate $R_{\rm tun}(E(t)) = \frac{4}{E(t)} \exp(-\frac{2}{3}\frac{1}{E(t)})$.

in the introduction, the adiabatic ionization is characterized by a dependence on the instantaneous field. Because of this field-history-independent nature of the adiabatic ionization, the total ionization probability remains the same whether an $E(t,\phi_0)$ pulse or a time-reversal $E(-t,\phi_0)$ pulse is applied. On the other hand, for any laser pulse with symmetric envelopes (as in the calculations of this paper), the time-reversal field corresponds to the CEP reversal field with $E(-t,\phi_0) = E(t,-\phi_0)$ (as long as pulses with $\phi_0 = 0$ correspond to the cosinelike pulses). Thus, in this case, a sign change of the CEP should not change the total ionization probability. This characteristic of the adiabatic ionization is clearly shown in Fig. 3(b) with the ionization probability to be distributed symmetrically according to the axis $\phi_0 = 0$. However, as we find in Fig. 3(a), this characteristic symmetry for adiabatic ionization disappears. The peaks that are supposed to be at $\phi_0 = 0$ gradually shift to the right as the pulse width decreases. This is a clear demonstration of the transfer from the adiabatic ionization channel to the nonadiabatic one.

For a pulse duration longer than the half cycle, the adiabatic ionization is still overwhelming and the main characteristics of the adiabatic ionization can still be identified: approximately symmetrical according to axis $\phi_0 = 0$ and bigger ionization probability for longer pulses [comparing the probability of 0.5 cycles to 0.6 cycles in Fig. 3(a)]. For even shorter pulses, bound electrons that escape from the adiabatic channel are sure to decrease gradually as predicted by adiabatic theory and shown in Fig. 3(b). Thus, any abnormal increase of the ionization probability should only be attributed to the nonadiabatic channel. This is exactly what happens in the sub-half-cycle region: as shown by Fig. 3(a), a shorter pulse with the same peak intensity as the longer ones, and thus less energy, could surprisingly have a much bigger ionization probability. This abnormal increase of the ionization probability implies that the nonadiabatic ionization could be very important when pulse width is in the sub-half-cycle region.

The breakdown of the symmetric pattern in Fig. 3(a) actually implies that the time reversal of the laser fields can change the final ionization yields. This field-history-dependent nature of the nonadiabatic ionization is out of the reach of any adiabatic theory. The instantaneous ionization rate with an adiabatic tunneling view, such as the Ammosov-Delone-Krainov (ADK) rate [27,28], can hardly explain this dependence. Even the more recent Yudin-Ivanov (YI) model [29], which includes the contribution from direct multiphoton ionization, may still fail to cover the corner. Rather than tunneling or direct multiphoton ionization from the initial state, the nonadiabatic ionization implies that there could be a third possibility: the bound electron may climb up the energy ladder and finally get ionized from a certain bound state other than the original one. Since the pulses are far from resonance with the atom, the multiphoton transitions between bound states must have played important roles. As pulse width decreases from 0.4 to 0.3 cycle, the spectra of the pulses may expand into a resonant area of multiphoton transition and it would not be really surprising to find a quick opening of the nonadiabatic ionization channels [Fig. 3(a)]. However, a detailed model of the process could be complex, as multienergy levels could have been involved. To model the nonadiabatic ionization process,

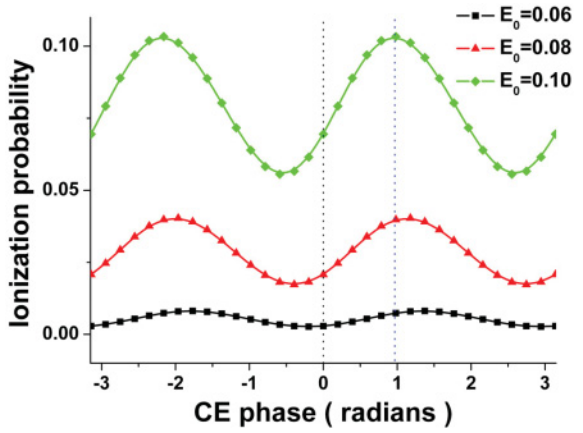

FIG. 4. (Color online) The TDSE results of total ionization probability vs CEPs for a hydrogenlike atom at ground state interacting with intense subcycle pulses with pulse intensity changing from 0.06 to 0.10 a.u.

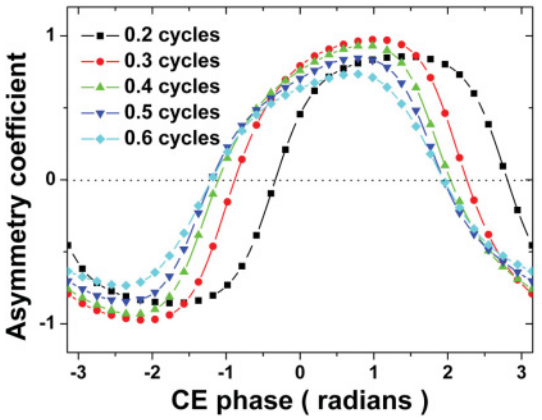

FIG. 5. (Color online) The asymmetry coefficient as a function of CEP obtained by TDSE with pulse width varying from 0.2 to 0.6 cycles.

one also needs to take into account the coherent population transfer by the ultrabroadband subcycle pulses [30,31].

Furthermore, the amount of the shift of the curves is generally a function of the intensity (Fig. 4). As the amplitude increases from 0.06 a.u. (1.26×10^{14} W/cm^2) to 0.10 a.u. (3.51×10^{14} W/cm^2), the shift of the curve from the origin decreases while the level of the ionization increases as expected. The dependence of the shift of the curve on the intensity is explainable. As intensity goes up to 3.51×10^{14} W/cm^2, the tunneling rate increases dramatically. As a result, this contribution from the adiabatic channel tends to drive the curve back to the symmetric position shown in Fig. 3(b).

B. The asymmetry of photoelectrons

The asymmetries of angular distributions of photoelectrons are a function of the CEP for few-cycle pulses because of the inversion asymmetry of the waveform [22]. It will surely remain true for subcycle pulses. In this paper, we focus on the role of the symmetry phase ϕ_s at which the number of photoelectrons going to the left equals to the number going to the right [$a(\phi_s) = 0$]. The symmetric phase has been found to be important [22]. It gives detailed information about the ionization process.

In the few-cycle cases, while the strong-field approximation (SFA) theory predicts $\phi_s = 0 \bmod \pi$, it has been found in marked contrast to be $\phi_s \sim -\frac{\pi}{3} \bmod \pi$ for intensity between 1×10^{13} W/cm^2 and 1×10^{14} W/cm^2 when calculated via solution of the TDSE [32]. These conclusions were confirmed by semiclassical methods [33] and the anti-intuitive symmetric phase is explained to be the result of the long-range Coulomb effect in detail [22,33].

In the subcycle region, this symmetric phase is still around $\phi_s \sim -\frac{\pi}{3} \bmod \pi$ for pulses longer than a half cycle. However, as shown by Fig. 5, it shifts dramatically to the right when the pulse width decreases from a half cycle to 0.2 cycle.

Again, to explain this shift of the symmetric phase, we need to take new effects into account. However, this time, it is not the Coulomb force but the nonadiabatic ionization process which should take responsibility. While the long-range Coulomb force scatters the photoelectrons that return to the core but lets go the directly ionized ones, thus resulting in the shift of the symmetric phase, the nonadiabatic ionization process changes the birth rate of the directly ionized electrons versus the returning ones. In the adiabatic regime, this rate has been supposed to be 1 for cosinelike pulses. In the nonadiabatic region, the leading part of the pulse will still directly ionize the electrons. What makes an important difference is that it may also drive the atoms to higher energy states [21]. Atoms in higher energy states are much easier to ionize than those in the original ground state. So the later part of the pulse will take advantage of that and the yield of the returning photoelectrons will increase. Thus, by suppression of the direct photoelectrons and increasing the returning ones, the symmetric phase tends to return to $\phi_s = 0 \bmod \pi$. This results in a shift of the CEP-dependent momentum asymmetry to the right as shown in Fig. 5. In this case, the symmetric phase again proves its importance in giving detailed information about the ionization processes.

IV. CONCLUSIONS

We studied the interaction of the intense subcycle pulses with a hydrogenlike system by solving the TDSE numerically. The results show that the nonadiabatic ionization process becomes very important when the pulse width is in the half-cycle region. And it leaves significant fingerprints in CEP-sensitive phenomena. For the description of the subcycle pulses, the vector-potential definition is found to be inadequate. Alternatively, we have presented an accurate expression for subcycle pulse with arbitrary pulse width.

ACKNOWLEDGMENTS

This work was supported by the National Nature Science Foundation of China (Grant No. 60925022), the Open Fund of the State Key Laboratory of High Field Laser Physics (Shanghai Institute of Optics and Fine Mechanics), and the Open Fund of the State Key Laboratory of Precision Spectroscopy (East China Normal University).

[1] P. B. Corkum and F. Krausz, Nat. Phys. **3**, 381 (2007).
[2] T. Brabec and F. Krausz, Rev. Mod. Phys. **72**, 525 (2000).
[3] D. You, R. R. Jones, P. H. Bucksbaum, and D. R. Dykaar, Opt. Lett. **18**, 290 (1993).
[4] M. Y. Shverdin, D. R. Walker, D. D. Yavuz, G. Y. Yin, and S. E. Harris, Phys. Rev. Lett. **94**, 033904 (2005).
[5] W. J. Chen *et al.*, Phys. Rev. Lett. **100**, 163906 (2008).
[6] G. Sansone *et al.*, Science **314**, 443 (2006).
[7] E. Goulielmakis *et al.*, Science **320**, 1614 (2008).
[8] A. E. Kaplan, J. Opt. Soc. Am. B **15**, 951 (1998).
[9] M. A. Porras, Phys. Rev. E **58**, 1086 (1998).
[10] S. M. Feng, H. G. Winful, and R. W. Hellwarth, Phys. Rev. E **59**, 4630 (1999).
[11] S. M. Feng and H. G. Winful, Phys. Rev. E **61**, 862 (2000).
[12] Z. Ulanowski and I. K. Ludlow, Opt. Lett. **25**, 1792 (2000).
[13] P. Saari, Opt. Express **8**, 590 (2001).
[14] Z. Wang, Q. Lin, and Z. Wang, Phys. Rev. E **67**, 016503 (2003).
[15] T. Brabec and F. Krausz, Phys. Rev. Lett. **78**, 3282 (1997).
[16] Q. Lin, J. Zheng, and W. Becker, Phys. Rev. Lett. **97**, 253902 (2006).
[17] I. P. Christov, Opt. Lett. **24**, 1425 (1999).
[18] K. Burnett, V. C. Reed, and P. L. Knight, J. Phys. B **26**, 561 (1993).
[19] M. Lewenstein, P. Balcou, M. Y. Ivanov, A. L'Huillier, and P. B. Corcum, Phys. Rev. A **49**, 2117 (1994).
[20] I. P. Christov, J. Zhou, J. Peatross, A. Rundquist, M. M. Murnane, and H. C. Kapteyn, Phys. Rev. Lett. **77**, 1743 (1996).
[21] I. P. Christov, M. M. Murnane, and H. C. Kapteyn, Phys. Rev. Lett. **78**, 1251 (1997).
[22] D. B. Milošević, G. G. Paulus, D. Bauer, and W. Becker, J. Phys. B **39**, R203 (2006).
[23] G. G. Paulus, F. Lindner, H. Walther, A. Baltuška, E. Goulielmakis, M. Lezius, and F. Krausz, Phys. Rev. Lett. **91**, 253004 (2003).
[24] Q. Lin, J. Zheng, Jianming Dai, I. Chen Ho, and X.-C. Zhang, Phys. Rev. A **81**, 043821 (2010)
[25] M. D. Feit *et al.*, J. Comput. Phys. **47**, 412 (1982).
[26] S. C. Rae, X. Chen, and K. Burnett, Phys. Rev. A **50**, 1946 (1994).
[27] M. V. Ammosov, N. B. Delone, and V. P. Krainov, Sov. Phys. JETP **64**, 1191 (1986).
[28] P. B. Corkum, Phys. Rev. Lett. **71**, 1994 (1993).
[29] G. L. Yudin and M. Y. Ivanov, Phys. Rev. A **64**, 013409 (2001).
[30] T. Nakajima and S. Watanabe, Phys. Rev. Lett. **96**, 213001 (2006).
[31] L. Chuntonov, A. Fleischer, and Z. Amitay, Opt. Express **19**, 6865 (2011).
[32] S. Chelkowski, A. D. Bandrauk, and A. Apolonski, Phys. Rev. A **70**, 013815 (2004).
[33] S. Chelkowski and A. D. Bandrauk, Phys. Rev. A **71**, 053815 (2005).